

## Microwave determination of the quasiparticle scattering time in $\text{YBa}_2\text{Cu}_3\text{O}_{6.95}$

D.A. Bonn, Ruixing Liang, T.M. Riseman, D.J. Baar, D.C. Morgan,  
Kuan Zhang, P. Dosanjh, T.L. Duty, A. MacFarlane, G.D. Morris, J.H. Brewer,  
and W.N. Hardy

*Department of Physics, University of British Columbia, Vancouver, British Columbia, Canada V6T 1Z1*

C. Kallin and A.J. Berlinsky

*Institute for Materials Research and Department of Physics and Astronomy, McMaster University, Hamilton,  
Ontario, Canada L8S 4M1*

(Received 9 April 1992)

We report microwave surface resistance ( $R_s$ ) measurements on two very-high-quality  $\text{YBa}_2\text{Cu}_3\text{O}_{6.95}$  crystals which exhibit extremely low residual loss at 1.2 K ( $2 - 6 \mu\Omega$  at 2 GHz), a broad, reproducible peak at around 38 K, and a rapid increase in loss, by 4 orders of magnitude, between 80 and 93 K. These data provide one ingredient in the determination of the temperature dependence of the real part of the microwave conductivity,  $\sigma_1(T)$ , and of the quasiparticle scattering time. The other necessary ingredient is an accurate knowledge of the magnitude and temperature dependence of the London penetration depth,  $\lambda(T)$ . This is derived from published data, from microwave data of Anlage, Langley, and co-workers and from high-quality  $\mu\text{sr}$  data. We infer, from a careful analysis of all available data, that  $\lambda^2(0)/\lambda^2(T)$  is well approximated by the simple function  $1 - t^2$ , where  $t = T/T_c$ , and that the low-temperature data are incompatible with the existence of an  $s$ -wave, BCS-like gap. Combining the  $R_s$  and  $\lambda(T)$  data, we find that  $\sigma_1(T)$  has a broad peak around 32 K with a value about 20 times that at  $T_c$ . Using a generalized two-fluid model, we extract the temperature dependence of the quasiparticle scattering rate which follows an exponential law,  $\exp(T/T_0)$ , where  $T_0 \approx 12$  K, for  $T$  between 15 and 84 K. Such a temperature dependence has previously been observed in measurements of the nuclear spin-lattice relaxation rate. Both the uncertainties in our analysis and the implications for the mechanism of high-temperature superconductivity are discussed.

### I. INTRODUCTION

Shortly after the discovery of high-temperature superconductivity<sup>1</sup> it was realized that even the normal state properties of the oxide superconductors are quite unusual. In particular the suggestion was soon made<sup>2</sup> that in order to understand the microscopic mechanism of the superconductivity it was first necessary to come to grips with these peculiar normal state properties, the most striking of which is the linear temperature dependence of the resistivity, which persists to surprisingly high temperatures and which, in the best samples, extrapolates to a very small intercept at  $T = 0$ . Also, in the far-infrared, a narrow Drude-like feature is observed, superimposed on a relatively temperature independent mid-infrared absorption.<sup>3</sup> The temperature dependence of the Drude peak indicates that a quasiparticle scattering rate,  $1/\tau(T)$ , that varies linearly with temperature is responsible for the linear temperature dependence of the dc resistivity.<sup>4</sup> It has been argued that the linear temperature dependence of the resistivity can be attributed to scattering by antiferromagnetic spin fluctuations<sup>5</sup> and experiments such as NMR (Refs. 6 and 7) and neutron scattering<sup>8</sup> have demonstrated the existence, in high- $T_c$  superconductors, of strong antiferromagnetic fluctuations. The presence of such fluctuations in these ma-

terials is not surprising in light of the fact that their undoped, "parent" compounds are antiferromagnetic insulators. What neutron scattering and magnetic resonance show is that the interactions which drive antiferromagnetism in the insulating state also have important consequences for the metallic phase.

The subject of this paper is the anomalous *superconducting* properties of high-temperature superconductors, particularly those of the best-studied compound,  $\text{YBa}_2\text{Cu}_3\text{O}_{7-\delta}$ . We report the results of a lengthy series of microwave surface resistance ( $R_s$ ) measurements on small  $\text{YBa}_2\text{Cu}_3\text{O}_{6.95}$  crystals of unusually high quality. Using published data for the imaginary part of the conductivity,  $\sigma_2(T)$ , we extract from  $R_s$  the temperature dependence of the real part,  $\sigma_1(T)$ , between 1.2 K and  $T_c$ . On the basis of a generalized two-fluid model<sup>9</sup> for the conductivity of a superconductor, we extend our analysis to obtain the temperature dependence of the quasiparticle scattering rate from  $T_c$  down to 1.2 K. We find that below  $T_c$  the scattering rate drops precipitously by about 3 orders of magnitude in such a way that its logarithm is fairly linear in  $T$  at least over the range from 15 to 84 K. This temperature dependence of the charged-quasiparticle scattering rate is identical to the temperature dependence found in all reported measurements of the nuclear spin-lattice relaxation rate be-

low  $T_c$ .<sup>6</sup> We argue from this fact and from the detailed temperature dependences of  $\lambda$  and  $\sigma$  that the dominant mechanism for charged-quasiparticle scattering is electronic spin-fluctuations. Our results for  $\tau(T)$  are consistent with the conductivity measurements of Nuss *et al.* at terahertz frequencies<sup>10</sup> and with the infrared results of Tanner and co-workers who were able to measure the quasiparticle conductivity in  $\text{Bi}_2\text{Sr}_2\text{CaCu}_2\text{O}_8$  in a relatively narrow range below  $T_c$ .<sup>11</sup> They are also strikingly similar to results for the temperature dependence of the vortex viscosity between 20 and 80 K in  $\text{Bi}_2\text{Sr}_2\text{CaCu}_2\text{O}_8$  crystals at microwave frequencies which have been measured in our lab and which will be published elsewhere.

In the two-fluid model of superconductivity used here, the conductivity is written as a sum of superconducting and normal parts. The superconducting part consists of a real  $\delta$  function at  $\omega = 0$ , together with its corresponding imaginary part, both weighted with the “superfluid fraction,”  $x_s(T) = 1 - x_n(T)$  where  $x_n(T)$  is the corresponding normal fraction. The normal fluid results from thermal excitations from the condensate. The response of the superfluid fraction is responsible for the screening of applied fields and its temperature dependence determines the temperature dependence of  $\sigma_2(T)$ , the microwave surface reactance and the London penetration depth,  $\lambda(T)$ . The relationships between these quantities allow one to use measurements of  $\lambda(T)$  in order to extract  $\sigma_1(T)$  from surface resistance measurements.  $\sigma_1(T)$  is determined by the response of the normal fluid and its temperature dependence is affected by the temperature dependence of both  $1/\tau(T)$  and  $x_n(T)$ . Thus, in order to extract the scattering rate from  $\sigma_1(T)$ ,  $x_n(T)$  must be inferred from  $x_s(T)$  and this requires very accurate knowledge of  $\lambda(T)$ , particularly at low  $T$ . Consequently, as part of the analysis of the microwave conductivity, it was necessary to reanalyze the best available data for the temperature dependence of  $\lambda(T)$ . This analysis yielded the surprising and simple result  $x_n(t) = t^2$  for  $0 < t < 1$ , where  $t \equiv T/T_c$ , suggesting the existence of low-lying states which might arise from nodes in the superconducting gap function or possibly from collective excitations. The fact that such a simple power law can be used to describe  $x_n(t)$  and hence the penetration depth for the entire temperature range below  $T_c$  is also surprising, although we are not the first to draw this conclusion.<sup>12</sup>

The remainder of this paper is organized as follows: Section II contains details regarding crystal growth and characterization and a description of the microwave technique along with the experimental data. A comparison is made between the surface resistance of two crystals measured at slightly different frequencies in order to assess the consistency of the measurements. Section III A reviews the relationship between the surface resistance  $R_s$ , the complex conductivity  $\sigma$ , and the London penetration depth  $\lambda$ . After a detailed discussion of microwave and  $\mu\text{sr}$  measurements of  $\lambda(T)$  in Secs. III B and III C, respectively, and discussion of the absolute values of  $T_c$  and  $\lambda(0)$  in Sec. III D, results for the temperature dependence of the conductivity of our crystals are presented in Sec. III E. In Sec. IV A we discuss the generalized two-fluid model in more detail in the context of weak-coupling BCS

theory and present our results for the temperature dependence of  $1/\tau(T)$  in Sec. IV B. Section V contains our conclusions and a discussion of what they tell us about the mechanism for high-temperature superconductivity.

## II. EXPERIMENT

The high-quality crystals used in the measurements presented here were grown by a flux technique described in detail elsewhere.<sup>13</sup> The attributes of these crystals that are most relevant to microwave measurements are clean, specular surfaces and a high degree of purity and homogeneity. High purity is achieved by the use of zirconia crucibles. The purity of the crystals was evaluated by ion conductive plasma mass spectroscopy and it was found that the total concentration of the principal contaminants, Al, Fe, and Zn, was less than 0.002 atoms/unit cell. Homogeneous oxygen content is particularly important in  $\text{YBa}_2\text{Cu}_3\text{O}_{7-\delta}$  because  $T_c$  is very sensitive to the oxygen stoichiometry. The crystals described here were annealed for 7 days in oxygen and the oxygen content was set at 6.95 ( $\delta = 0.05$ ) using the empirical relationship between annealing temperature, oxygen partial pressure, and  $\delta$  determined by Schleger *et al.*<sup>14</sup> This oxygen content yields a  $T_c$  near 93 K and outstanding bulk homogeneity is demonstrated by a specific heat jump at  $T_c$  that is very narrow, only 0.2 K wide. The transition measured by magnetic susceptibility in a field along the  $c$  axis is typically less than 2 K wide (10–90%) for a field of 100 G, and approaches the width of the specific heat jump as the field is reduced below a few gauss. The microwave loss itself is perhaps the most stringent test of a crystal’s quality and the manner in which inhomogeneity and dirty or damaged surfaces might affect the measurements will be discussed below.

The surface resistance of the crystals was measured near 2 GHz by cavity perturbation of a superconducting split-ring resonator with a high-quality factor ( $Q$ ).<sup>15</sup> This technique allows accurate measurement of a very wide range of microwave losses in very small crystals. The measurements are performed by introducing a sample, mounted on a sapphire rod, along the axis of the resonator where microwave magnetic fields drive currents in the  $ab$  plane of the crystal. The difference between the cavity  $Q$  with the sample in ( $Q_s$ ) and the  $Q$  with the sample out ( $Q_o$ ) is used to determine the surface resistance ( $R_s$ ) via

$$R_s = A\Delta(1/Q) = A[1/Q_s - 1/Q_o], \quad (1)$$

where  $A$  is a constant that depends on the area and position of the sample. Thus, measurement of low losses depends on accurate measurement of  $Q$ ’s and a large value of  $Q_o$ . The split-ring resonator used in the measurements presented here had a  $Q$  of  $2 \times 10^6$  at 1.2 K which could be measured with an accuracy of  $\pm 0.2\%$ .<sup>15</sup> A value of  $\Delta(1/Q)$  typically measured in a small crystal of  $\text{YBa}_2\text{Cu}_3\text{O}_{6.95}$  at low temperature is  $2 \times 10^{-8}$  with an estimated uncertainty of 10% .

The calibration constant,  $A$ , can be determined by measurement of  $\Delta(1/Q)$  for a sample with a known sur-

face resistance. This calibration has been performed with a piece of electropolished stainless steel but with only limited accuracy because of the difficulty of cutting a piece of stainless steel that is the same size and shape as the small crystals of  $\text{YBa}_2\text{Cu}_3\text{O}_{6.95}$ . A much more accurate way of determining the calibration constant is to compare the normal state microwave loss measurements to dc resistivity measurements. Far-infrared measurements indicate that at low frequencies the optical absorption of  $\text{YBa}_2\text{Cu}_3\text{O}_{7-\delta}$  in the normal state is consistent with the classical skin effect,<sup>3</sup> thus, the microwave surface resistance should follow the relation

$$R_s(T) = \left( \frac{2\pi\rho_{\text{dc}}\omega}{c^2} \right)^{1/2}, \quad (2)$$

where  $\rho_{\text{dc}}$  is the dc resistivity,  $\omega$  is the angular frequency, and  $c$  is the speed of light in free space. (Throughout this paper, cgs units will be employed. The relevant conversion factor is  $9 \times 10^{11} \Omega = 1 \text{ s/cm.}$ ) Direct dc resistivity measurements in the  $ab$  plane have been performed on crystals from the same batch as those used in the microwave measurements. Calibration of the surface resistance measurements is then simply a matter of using the measured dc resistivity to calculate the surface resistance at a convenient temperature (100 K) via Eq. (2), where

$$A = \frac{(2\pi\rho_{\text{dc}}(100 \text{ K})\omega/c^2)^{1/2}}{\Delta(1/Q)|_{T=100 \text{ K}}}. \quad (3)$$

Figure 1 compares the measured dc resistivity to the square of the calibrated measurements of surface resistance.

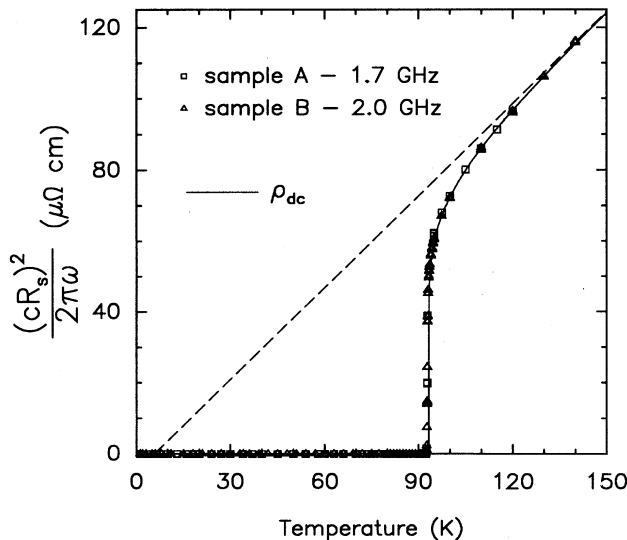


FIG. 1. The square of the surface resistance of two crystals of  $\text{YBa}_2\text{Cu}_3\text{O}_{6.95}$  compared to the  $ab$ -plane resistivity of a crystal produced in the same flux growth. The microwave results are set equal to  $\rho_{\text{dc}}$  at 100 K. The close agreement between the measurements over a wide range of temperatures supports the use of the classical skin effect expression for the normal state surface resistance to calibrate the microwave measurements.

tance for two crystals of  $\text{YBa}_2\text{Cu}_3\text{O}_{6.95}$ . Sample A, measured at 1.7 GHz, was an 8-mm<sup>2</sup> crystal with a relatively high twin density (twin spacing  $< 1 \mu\text{m}$ ) and sample B, measured at 2.0 GHz, was a small, nearly twin-free corner broken off of the same crystal. The good agreement at all temperatures above  $T_c$  in Fig. 1 indicates that the calibration at 100 K is a reasonable one. As is observed in the dc resistivity, the square of the surface resistance in the normal state falls below the linear temperature dependence as the superconducting transition is approached. This behavior is generally attributed to 2D superconducting fluctuations<sup>16</sup> and we find<sup>17</sup> that the departure from linearity is reasonably well described above 94 K by the 2D fluctuation model of Aslamazov and Larkin.<sup>18</sup>

The full temperature dependence of the surface resistance of crystals A and B is displayed in a semi-log graph in Fig. 2. The qualitative features are the same as those found in a preliminary study of a crystal grown by a somewhat different flux technique.<sup>19</sup> After a rapid drop below  $T_c$  of 4 orders of magnitude the loss rises slightly to a broad maximum near 38 K and then falls again at lower temperatures. There are very few microwave loss studies of crystals of  $\text{YBa}_2\text{Cu}_3\text{O}_{7-\delta}$  with which to compare these results. The cavity perturbation studies of Wu *et al.*<sup>20</sup> at 10 GHz and Rubin *et al.*<sup>21</sup> at 5.95 GHz could not resolve losses below 0.4 and 1.0 mΩ/□, respectively, limiting their measurements of temperature dependence to the vicinity of the superconducting transition. Rubin

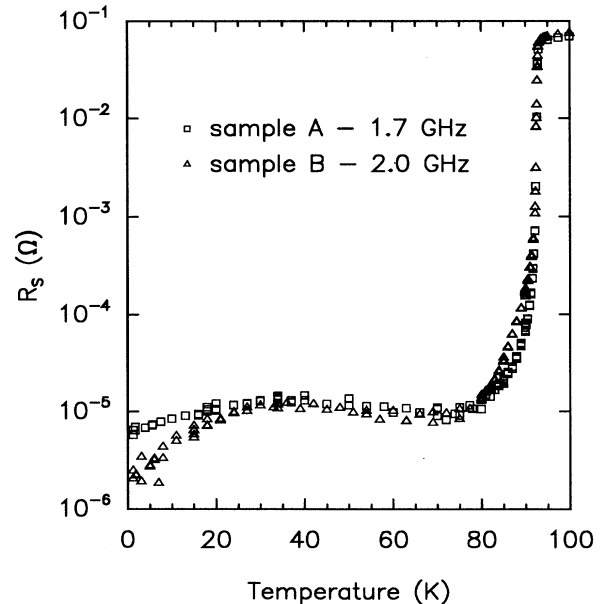


FIG. 2. The surface resistance of two crystals of  $\text{YBa}_2\text{Cu}_3\text{O}_{6.95}$ . Although the two samples exhibit somewhat different transition widths and quite different low temperature residual loss, the qualitative features of the measurements are the same. Both have a large drop in loss of 4 orders of magnitude at  $T_c$  and an unusual nonmonotonic temperature dependence at lower temperatures.

*et al.* also used a calorimetric technique to establish an upper limit of  $15 \mu\Omega/\square$  for the loss of a mosaic of crystals at 4.2 K. This is in reasonable agreement with the measurements presented here, although the loss at this low temperature is probably strongly influenced by extrinsic factors.

There are two noteworthy differences between the two data sets in Fig. 2. First, sample B appears to have a somewhat broader transition than sample A; there is a broad tail extending down to 84 K. While it is natural to consider the sharper transition to be closer to the intrinsic temperature dependence of the loss, this difference between the two measurements should prompt one to exercise caution in the interpretation of microwave measurements near  $T_c$ . Because the loss initially drops very rapidly, a small degree of inhomogeneity could lead to a substantial change in the appearance of the transition on a logarithmic scale. It is possible that a measurement of the transition by surface resistance is a particularly stringent test of a sample's degree of homogeneity. The second difference between the two measurements is in the residual loss measured at the lowest temperatures. The residual loss of sample A is  $6 \mu\Omega/\square$  but that of sample B is only  $2 \mu\Omega/\square$ , the latter value being near the limit of what can be resolved with this experimental technique. It is tempting to associate the higher residual loss in sample A with the higher degree of twinning, but the more mundane explanation of damage or dirt on the surface can only be ruled out by changing the degree of twinning in a sample and remeasuring its loss.

Residual loss is a long-standing problem in microwave studies of superconductors.<sup>22</sup> Given a sufficiently sensitive microwave technique the measurement of intrinsic temperature dependent loss is largely reduced to the materials problem of reducing residual loss. Rather few of the hundreds of crystals that have been grown with the technique outlined in Ref. 13 are suitable for microwave studies. Many crystals have some residual flux on the surface, or cracks on the edge, or growth steps, all of which might contribute to large residual losses. Of the 8 crystals that we have studied so far, 4 had a residual loss high enough to obscure the nonmonotonic temperature dependence, 3 had a residual loss comparable to that of crystal A, and crystal B exhibited the lowest residual loss that we have observed. Traditionally, the low temperature residual loss is subtracted from the entire data set in order to extract the temperature dependent part. This approach, which is one of the two techniques used in the following analysis, ignores the possibility of intrinsic residual loss, a possibility which will also be considered in the analysis that follows.

Figure 3 displays in detail the loss below  $T_c$  of crystals A and B after subtraction of residual loss. Assuming that the intrinsic loss varies as  $\omega^2$ , as is the case in the two-fluid model, the data for sample A has been scaled up by 38% in order to account for the difference in frequency of the two measurements. The decrease in the scatter in the data below 20 K is due to a slight difference in the measurement procedure above and below this temperature. Above 20 K the measurements are made by ramping up and down in temperature over a period of 2–3 days. Be-

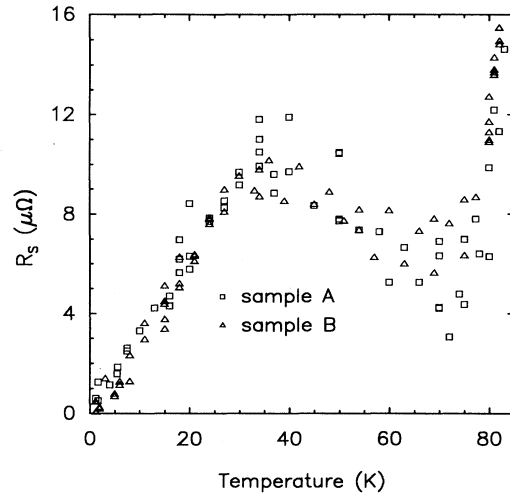


FIG. 3. The surface resistance at 2 GHz of two crystals of  $\text{YBa}_2\text{Cu}_3\text{O}_{6.95}$  in the low loss regime. The low temperature residual loss in Fig. 2 has been subtracted from the data and the measurements for sample A have been scaled up by 38% in order to account for the different frequencies used in the two sets of measurements. The broad peak centered at 38 K and the nearly linear temperature dependence below 30 K are reproducible from sample to sample.

low 20 K, cooling is achieved by gradually introducing helium exchange gas into the sample area and the data is taken over a few hours and only in one direction. The excellent overall agreement in Fig. 3 strongly suggests that the nonmonotonic temperature dependence of the surface resistance at 2 GHz is intrinsic. Another striking feature of the measurements is the apparent linearity of the data below 30 K. Neither this linearity nor the nonmonotonic behavior are features that are observed in conventional low- $T_c$  superconductors.

### III. EXTRACTING THE CONDUCTIVITY FROM $R_s$

#### A. Local electrodynamics

In  $\text{YBa}_2\text{Cu}_3\text{O}_{7-\delta}$  the mean-free path in the  $c$ -axis direction is considerably shorter than either the normal state skin depth or the London penetration depth. In this situation the low frequency electrodynamic properties are local and the surface resistance can be written in terms of the complex resistivity as<sup>23</sup>

$$R_s = \sqrt{\frac{2\pi\omega}{c^2} (|\rho| + \rho_2)}, \quad (4)$$

where

$$\rho = \rho_1 + i\rho_2 = \frac{1}{\sigma_1 + i\sigma_2}. \quad (5)$$

Instead of using the quantity  $R_s$ , we work with a con-

ductivity,  $\sigma_s$ , defined as

$$\sigma_s = \frac{2\pi\omega}{c^2 R_s^2}, \quad (6)$$

which is the real conductivity corresponding to  $R_s$  when  $\sigma_2 = 0$ . Equation (4) can then be rewritten as

$$\frac{1}{\sigma_s} = \frac{1}{\sqrt{\sigma_1^2 + \sigma_2^2}} - \frac{\sigma_2}{\sigma_1^2 + \sigma_2^2}, \quad (7)$$

which, if  $\sigma_2$  is known, is equivalent to a quadratic equation for the quantity  $\sqrt{\sigma_1^2 + \sigma_2^2}$ , hence determining the value of  $\sigma_1$ . The result is

$$\sigma_1 = \sqrt{\left(\frac{\sigma_s}{2} \pm \sqrt{\frac{\sigma_s^2}{4} - \sigma_2\sigma_s}\right)^2 - \sigma_2^2}, \quad (8)$$

where the + (−) sign applies to the case  $\sigma_1 > (<)\sqrt{3}\sigma_2$ .

In the normal state, the conductivity is essentially real, i.e.,  $\sigma_2 = 0$  and  $\sigma_1 = \sigma_s$ . In the superconducting state,  $\sigma_2$  at microwave frequencies is completely dominated by the effect of the  $\delta$  function at the origin in  $\sigma_1$ . That is, the Kramers-Kronig relation connecting the real and imaginary parts of the conductivity implies that the delta function at the origin in the real part,  $\sigma_1(\omega, T) = \delta(\omega)c^2/8\lambda^2(T)$ , gives rise to the dominant term in the imaginary part of the conductivity<sup>24</sup> and can be written in terms of the penetration depth:

$$\sigma_2(\omega, T) = \frac{c^2}{4\pi\omega\lambda^2(T)}. \quad (9)$$

Except for a very narrow region just below  $T_c$ , the conditions  $\sigma_1 \ll \sigma_2 \ll \sigma_s$  are satisfied, and Eq. (8) can be expanded to give

$$\sigma_1 \approx \sqrt{\frac{2\sigma_2^3}{\sigma_s}}, \quad (10)$$

or, using Eqs. (6), (9), and (10),

$$\sigma_1 \approx \frac{R_s c^4}{8\pi^2 \omega^2 \lambda^3(T)}. \quad (11)$$

The exact expression, Eq. (8), is really only required in the very narrow temperature region, just below  $T_c$ , in which  $\sigma_2$  is comparable to  $\sigma_1$ . In our simple two-fluid picture, this corresponds approximately to the temperature range

$$\frac{T - T_c}{T_c} < \frac{\omega\tau}{2}. \quad (12)$$

For the frequencies of our experiments (1–3 GHz) and for our  $\text{YBa}_2\text{Cu}_3\text{O}_{6.95}$  crystals,  $\omega\tau \approx 10^{-3}$  at  $T_c$ , and so, the temperature region defined by Eq. (12) extends less than 0.1 K below  $T_c$ . Nevertheless we have in all cases used the full expression, Eq. (8), in our analysis of the data. On the other hand, Eq. (11) is particularly useful for understanding various trends in the analysis.

Data such as that shown in Figs. 2 and 3 can be analyzed using the exact relations, Eqs. (6) and (8), or

the approximate expression, Eq. (11). In either case, one must know the temperature-dependent penetration depth,  $\lambda(T)$ .

## B. The temperature dependence of $\lambda$

There have been many measurements of  $\lambda(T)$  by a variety of methods, including microwave techniques,<sup>12,25,26</sup> magnetic susceptibility,<sup>27</sup> kinetic inductance measurements,<sup>28</sup> and  $\mu\text{sr}$ .<sup>29,30</sup> These will be discussed in great detail below. The London penetration depth can be parametrized in terms of the normal fluid density by the expression

$$\lambda^{-2}(T) = \lambda^{-2}(0)[1 - x_n(T)] = \lambda^{-2}(0)x_s(T). \quad (13)$$

We will argue below that, to the accuracy of the available data,  $x_n(T)$  is given by

$$x_n(T) = (T/T_c)^2 \equiv t^2. \quad (14)$$

One motivation for measuring the temperature dependence of  $\lambda$  is that it sheds light on the underlying microscopic model. In particular, at low  $T$ , the small difference between  $\lambda(T)$  and its low temperature limiting value  $\lambda(0)$ ,

$$\Delta\lambda(t) = \lambda(t) - \lambda(0) \approx \frac{1}{2}\lambda(0)x_n(t), \quad (15)$$

depends on the density of low-lying states of the superconductor. If the superconductor has a nonzero gap, then  $x_n(T)$  will have an activated temperature dependence. On the other hand, if there are nodes in the gap or if the excitation spectrum from the condensate is gapless, then  $x_n(T)$  will follow some power law at low  $T$ .<sup>31</sup> The chief difficulty of interpreting measurements of  $\lambda(T)$  in terms of either of these scenarios is that very accurate measurements must be made in order to unambiguously determine the behavior of  $x_n(t)$ .

There have been many reports of power-law behavior for the low-temperature behavior of the penetration depth in  $\text{YBa}_2\text{Cu}_3\text{O}_{7-\delta}$ . Some of these are discussed in the paper by Annett *et al.*<sup>32</sup> who found that kinetic inductance measurements were best fit by the form

$$\frac{\Delta\lambda_{ab}(t)}{\lambda_{ab}(0)} = Bt^2 + \dots, \quad (16)$$

where  $t \equiv T/T_c$ . They obtained  $B = 0.63$  and 1.6 for the two films which they analyzed. We note that the value  $B = 0.5$  corresponds to  $x_n(t) = t^2$ .

More recently, two groups have studied the temperature dependence of the penetration depth in microstrip resonators. In the first of these, Anlage and co-workers<sup>26</sup> interpreted their data in terms of two BCS-like gaps,  $2\Delta(0)/kT_c = 4.5$  close to  $T_c$  and  $2\Delta(0)/kT_c = 2.5$  at lower temperatures. They also considered a weak link model of weakly coupled grains.

Subsequently Anlage *et al.*<sup>33</sup> have published results, for samples measured in a vacuum can, which suggest a smaller low temperature gap,  $2\Delta(0)/kT_c = 1.0$  or low temperature power-law behavior. They point out that early measurements of  $\lambda(T)$  were influenced by a temper-

ature dependent dielectric constant associated with the presence of helium vapor, leading to somewhat enhanced estimates of the low temperature energy gap. We have analyzed data, similar to that of Ref. 33, which were sent to us by the authors. The first step in this analysis consists of finding the most reasonable extrapolation to the phase velocity to  $T = 0$ . To motivate our extrapolation, we show the low temperature portion of this data set, plotted as phase velocity squared versus  $T^2$ , in Fig. 4. Also indicated in the figure are two possible extrapolations. The higher of these two extrapolations results in an approximate power-law dependence for  $\lambda(T)$  of the form

$$\frac{1}{\lambda^2(T)} = \frac{1}{\lambda^2(0)}(1 - bt^2). \quad (17)$$

In Fig. 5 the analyzed data (the dots), assuming  $\lambda(0) = 1450 \text{ \AA}$ , are compared with Eq. (17) with  $b=1$ . We note that the fact that the coefficient of  $t^2$  is the same over the entire range of temperatures is both remarkable and unexpected. Using the same  $\lambda(0)$  and the lower extrapolation from Fig. 4 leads to no visible difference in the fit above  $t = 0.6$ . Below  $t = 0.5$  the data lie about 1% above the curve  $1-t^2$ . Uncertainties in the interpretation of the above data arise from sample-dependent results, uncertainties in the value of the effective dielectric constant of the dielectric spacer in the microstrip, and other experimental problems which have been described elsewhere<sup>25</sup> by the authors.

We should emphasize that the interpretation by Anlage and co-workers of their data,<sup>26</sup> in terms of a large intrinsic gap and a smaller grain-boundary gap, has been the basis for the analysis of a large body of microwave, dc, and optical measurements performed on the same set of thin films.<sup>34</sup> Our approach provides an alternative interpretation of the data which can be tested by further measurements.

Some support for our interpretation can be found in the recent measurement by Pond *et al.*<sup>12</sup> of a trilayer

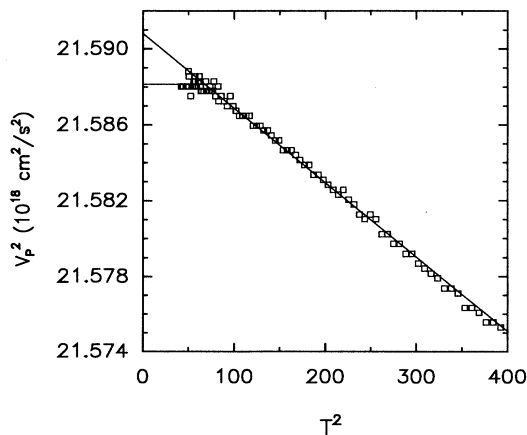


FIG. 4. The square of the phase velocity (squares) at low temperatures plotted versus the square of the temperature from the data of Langley *et al.* The solid lines represent two possible extrapolations of the data.

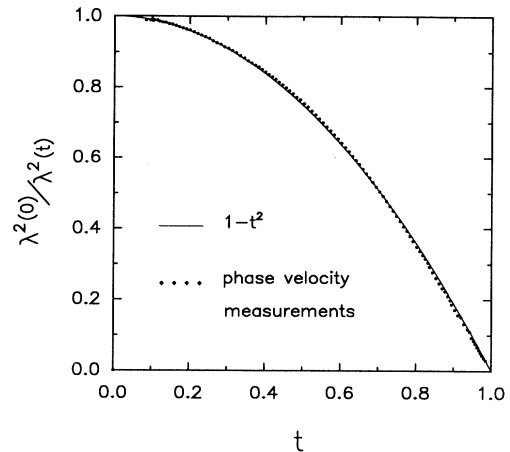


FIG. 5. The temperature dependence of the London penetration depth extracted from the phase velocity measurements shown in Fig. 4 using the upper extrapolation shown in that figure and taking  $\lambda(0) = 1450 \text{ \AA}$ .

transmission line resonator with a very thin ( $0.2\mu$ ) dielectric layer, a factor of 10 thinner than that used by Anlage *et al.*<sup>26</sup> The very large ratio of the width of the resonator to the dielectric layer thickness greatly suppresses the effects of fringing fields and dielectric shifts due to material external to the device, thus effectively removing a major source of uncertainty. Although they noted that their data could be fit by a BCS temperature dependence with  $\lambda(0) = 1350 \text{ \AA}$ , a noticeably better fit was obtained, particularly below  $T_c/2$ , using Eq. (17) with  $b = 1$  and  $\lambda(0) = 1300 \text{ \AA}$ . Unfortunately the data of Pond *et al.* extend only down to 20 K. It would be useful to have such high quality data at least down to 4.2 K to see whether the temperature dependence flattens out, as it would if there is a true gap, or whether the data continue to follow a  $T^2$  law.

### C. $\mu$ sr data

Another experiment that is used to determine the London penetration depth is muon spin relaxation ( $\mu$ sr). Here we present new results for such measurements and compare them to earlier work. The  $\mu$ sr measurements described below were performed on a mosaic of  $\text{YBa}_2\text{Cu}_3\text{O}_{6.95}$  crystals grown by the same technique as that used to produce crystals for the microwave measurements. The crystals were mounted on a disc of 99.9985 % Ag with Apiezon N grease. In order to probe the  $ab$ -plane penetration depth a static 0.25-T magnetic field is applied along the  $c$  axis so that when a muon, with its spin aligned perpendicular to the field, stops in the bulk of the sample it precesses at a rate proportional to the local field at the muon site. In a type-II superconductor the applied field sets up a vortex lattice which gives rise to a spatial distribution of internal local fields. In the isotropic, modified London model the spatial field distribution is given by<sup>35</sup>

$$B(\mathbf{r}) = B_{\text{av}} \sum_{\mathbf{K}} \frac{\exp(-i\mathbf{K} \cdot \mathbf{r})}{1 + K^2 \lambda^2} \exp\left(\frac{-K^2 \xi^2}{2}\right), \quad (18)$$

where  $B_{\text{av}}$  is the average field in the superconductor,  $\mathbf{K}$  is the set of reciprocal lattice vectors for the vortex lattice, and  $\xi$  is the coherence length. In the 0.25-T applied field used in this experiment  $K^2 \lambda^2 \gg 1$  and at temperatures below about 87 K,  $B(\mathbf{r}) - B_{\text{av}}$  is field independent and proportional to  $\lambda^{-2}$ . At higher temperatures consideration of the effect of  $\xi$  in Eq. (18) shows that the vortex cores take up an appreciable area and this straightforward relationship between  $\lambda$  and the fields is no longer true.<sup>36</sup>

The spatial distribution of internal magnetic fields manifests itself in a probability distribution of muon precession frequencies, the  $\mu\text{sr}$  line shape. The ideal line shape corresponding to the field distribution of Eq. (18) has, at a field lower than the applied field, a cusp-shaped maximum whose source is the saddle point in  $B(\mathbf{r})$  between adjacent pairs of vortices. Imperfections in the vortex lattice lead to smearing of this peak and can be modeled by convolving a Gaussian with the ideal line shape. A fit to a high statistics run taken at 10 K gives  $\lambda_{ab} = 1405 \pm 92$  Å and a Gaussian convolution of  $17.2 \pm 2.4$  G. In order to take into account flux expulsion below  $T_c$  this fit assumed that  $B_{\text{av}}$  was 3.8 G less than the 0.25-T applied field, a value that is taken from a fit to the temperature dependence of the  $\mu\text{sr}$  peak (see discussion below) and that is consistent with the expulsion observed in a SQUID measurement of the magnetization of one of the crystals used in the mosaic. Assuming a smaller flux expulsion of 0.5 G reduces the penetration depth by only half the statistical error.

The difference between the field corresponding to the cusp in the ideal line shape and  $B_{\text{av}}$  is proportional to  $\lambda^{-2}$ . The detailed fit at 10 K indicates that the Gaussian convolution shifts the peak of the  $\mu\text{sr}$  line shape from the ideal cusp in such a way that the difference between the average field and the field corresponding to the measured peak is 85% of the difference between the average field and the cusp of the ideal line shape. If the Gaussian convolution truly reflects the disorder in the vortex lattice due to pinning and is frozen in as the sample is field cooled through the irreversibility temperature (which is only a few degrees below  $T_c$ ), the size of the Gaussian convolution would have the same temperature dependence as  $\lambda^{-2}$ . In this case the difference between the measured peak and the average internal field is still proportional to  $\lambda^{-2}$ . So, for the purposes of determining the temperature dependence of  $\lambda$ , one can fit lower statistics data using a less computationally intensive function, provided that it gives an accurate measure of the position of the measured peak. We have chosen to fit with two Lorentzians (exponentials in time-space); one models the background signal for muons stopping in the silver disk rather than in the crystals and the other fits the superconductor's cusp peak well enough to give a good measure of the peak position. Fitting with two Gaussians was also tried, but the fits were much worse and the peak of the "sample" Gaussian did not correspond to the experimentally observed peak.

Figure 6 shows the difference between the applied field,  $B_{\text{ap}}$ , and the field that corresponds to the peak in the  $\mu\text{sr}$  signal coming from the sample,  $B_c(T)$ . The data was fit using

$$B_c(T) - B_{\text{ap}} = \delta B_c [1 - (T/T_c)^p] + \frac{2c_B}{\pi} \arctan[(T - T_c)/c_T] \quad (19)$$

between  $T = 5$  and  $T = 87$  K. The first term on the right-hand side of this expression is proportional to  $\lambda^{-2}(T)$  and we have chosen a power-law temperature dependence to see if the  $\mu\text{sr}$  measurements are consistent with the other measurements of  $\lambda(T)$  discussed above. The arctan function represents the temperature dependence of the flux expulsion, where  $c_T$  was fixed to a value of  $-1.24$  K from magnetization measurements and  $c_B$  was allowed to vary. Since we limited the fit to temperatures below 87 K, only the total amount of flux expulsion  $c_B$  is important in the determination of the temperature dependence of  $\lambda$ . With  $T_c$  fixed to the onset value of 93.5 K measured by specific heat, the fit gives a flux expulsion of  $c_B = -3.8$  G, a shift of the cusp from the average internal field of  $\delta B_c = -27.8 \pm 0.6$  G and a power  $p$  of  $2.37 \pm 0.10$ . This power is quite close to the  $t^2$  behavior observed in the phase velocity measurements described above.

The fact that this interpretation is at odds with other interpretations of  $\mu\text{sr}$  measurements<sup>30,29</sup> again highlights the problem that the crucial difference between power-law behavior and  $s$ -wave BCS theory occurs at temperatures below  $T_c/2$  where the temperature dependence of  $\lambda$  is relatively weak and difficult to measure with sufficient accuracy. The measurements of an oriented polycrystal by Pümpin *et al.*<sup>30</sup> are consistent with our data but they only show three data points below  $T_c/2$  and the

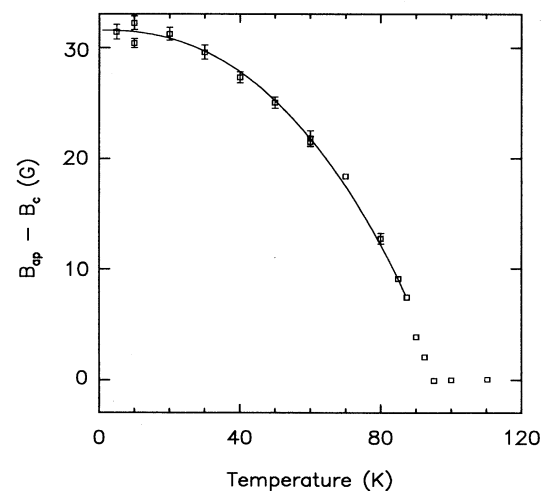


FIG. 6. The temperature dependence of the difference between the applied magnetic field,  $B_{\text{ap}}$ , and the field corresponding to the position of the maximum in the  $\mu\text{sr}$  line shape,  $B_c(T)$ , is a measure of the temperature dependence of  $\lambda^{-2}$ . The data (squares) is well fit by the solid line which is derived from Eq. (19) and corresponds to  $p = 2.37 \pm 0.10$ .

uncertainty in the data is too large to make any strong conclusion about the behavior of  $\lambda(T)$  at low temperatures. On the basis of measurements at six temperatures, only three of which were below  $T_c/2$ , Harshman *et al.*<sup>29</sup> claimed that the temperature dependence of  $\lambda(T)$  in the  $ab$  plane is consistent with  $s$ -wave BCS theory. Although the three low temperature points in their data set were relatively temperature independent, the sparseness of the data and a scatter of the data points which appears to be larger than the statistical error estimate makes the claim of  $s$ -wave BCS behavior a weak one. The more complete data set that we have presented is consistent with the power-law temperature dependence observed in the kinetic inductance and microwave measurements and exhibits too much temperature dependence below  $T_c/2$  to be consistent with  $s$ -wave BCS behavior.

#### D. The determination of $T_c$ and $\lambda(0)$

The use of Eqs. (13) and (14) to model  $\lambda(T)$  introduces two parameters,  $T_c$  and  $\lambda(0)$ , into the analysis of the surface resistance. We find that the value of  $T_c$  is quite accurately determined by our data, particularly for sample A which exhibits the sharper transition. Choosing  $T_c$  slightly too large or too small pulls  $\sigma_1(T < T_c)$  up or down quite noticeably, creating a spurious peak or dip just below the transition. The value  $T_c = 92.7$  K minimizes this tendency. However even for this value, there are four points between 92.2 and 92.9 K which form a very narrow peak. This peak indicates that, for one reason or another (perhaps because of sample inhomogeneity or thermal fluctuations), our model is inadequate within a few tenths of a degree of  $T_c$ . However, the condition that there be no anomalous dip or rise just below  $T_c$  suffices to determine a value of  $T_c$  to within  $\pm 0.2$  K. The 92.7 K  $T_c$  is 0.5 K below the value determined by magnetization and resistivity measurements, but this is probably due to some variation in thermometer calibration or a small thermal gradient.

The absolute value of  $\lambda(0)$  is more difficult to determine. The measurements discussed above most commonly yield a London penetration depth near 1450 Å.<sup>12,25–29</sup> In principle, analysis of the surface resistance measurements near  $T_c$  can also be used to make an estimate of  $\lambda(0)$  for the crystals used in the study described here, but broadening of the superconducting transition by fluctuations and sample inhomogeneity limit the usefulness of this approach. Throughout the remainder of this paper we will simply adopt a value of 1450 Å for  $\lambda(0)$  and point out that further improvements in sample quality and measurements at higher frequency may eventually lead to a reliable estimate of  $\lambda(0)$ .

#### E. The conductivity

Using the expressions for  $\sigma_1$  in Sec. III A [Eqs. (4)–(8)] and the temperature dependent London penetration depth discussed in detail in Secs. III B–III D one can extract the real part of the conductivity from the surface resistance. The results of the above analysis, including

the use of Eq. (14), are the conductivities shown in Figs. 7(a) and 7(b). Figure 7(a) is extracted directly from the data of Figs. 2 and 7(b) follows from analysis of the data after subtracting a sample dependent, temperature independent residual loss. In both cases the conductivity for sample B has an abrupt peak between  $T_c$  and 84 K that is nearly absent in sample A. This peak, which results from the broad tail in the transition in sample B, may be related to the sharp peak near  $T_c$  observed in some microwave measurements on films of  $\text{YBa}_2\text{Cu}_3\text{O}_{7-\delta}$ ,<sup>37</sup> crystals of  $\text{YBa}_2\text{Cu}_3\text{O}_{7-\delta}$ ,<sup>38</sup> and crystals of  $\text{Bi}_2\text{Sr}_2\text{CaCu}_2\text{O}_8$  (Ref. 39) in the 60-GHz range. In particular, Glass and Hall have used a model based on effective medium theory to calculate the effect of a broadened transition on the conductivity.<sup>40</sup> Their model suggests that the abrupt

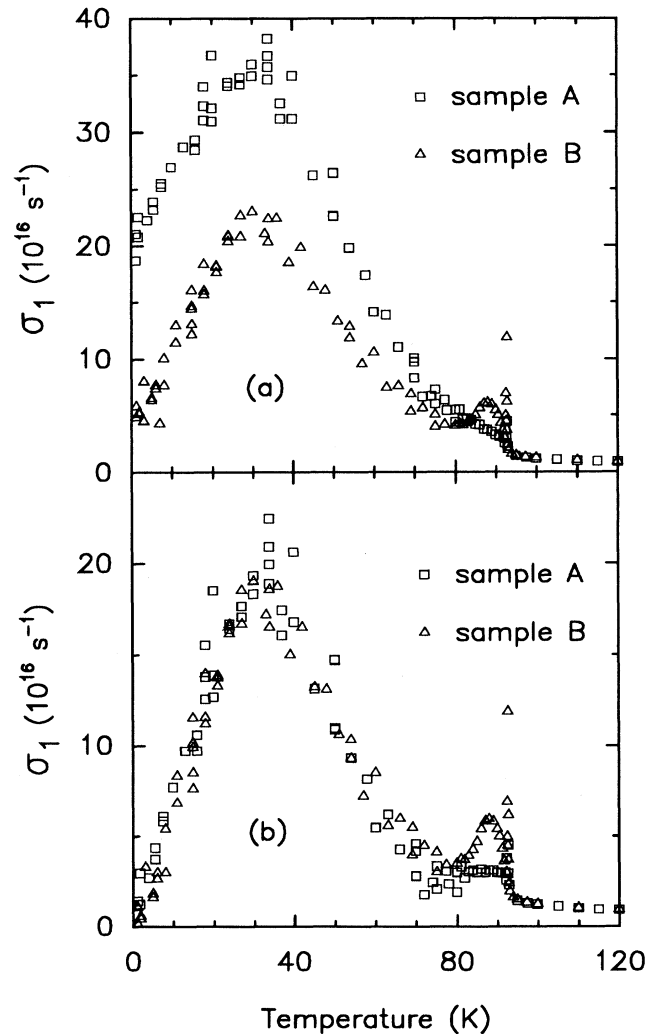


FIG. 7. The real part of the optical conductivity extracted from the surface resistance of crystals A and B; (a) shows the conductivity obtained directly from the surface resistance without subtracting any residual loss; (b) is obtained after subtracting a temperature independent loss of  $6 \mu\Omega$  for sample A and  $2 \mu\Omega$  for sample B.

rise in conductivity observed below  $T_c$  in a thin film of  $\text{YBa}_2\text{Cu}_3\text{O}_{7-\delta}$  (Ref. 37) might partly be the result of sample inhomogeneity. Despite the potential problem with interpreting the surface resistance near  $T_c$ , the measurements made on sample A seem to be close to intrinsic for temperatures a degree or more below  $T_c$ . Sample B is quite anomalous in our experience. The broad tail in its surface resistance is the largest that has been observed in any crystal grown by the technique described in Ref. 13 and this might be due to the fact that the sample was stressed when it was broken off of the corner of sample A.

The main effect of the subtraction of residual loss is to force the conductivity to approach zero at zero temperature, which is equivalent to forcing the normal fluid density to approach zero with decreasing temperature. It should be noted that the subtraction also has an effect on the qualitative behavior of the conductivity for  $T \approx 70$  K in sample A. When the residual loss is not subtracted, the resulting conductivity for sample A smoothly increases as the temperature falls below 80 K, as is observed in sample B whether its smaller residual loss is subtracted or not. However, when a  $6\text{-}\mu\Omega$  residual loss is subtracted from the surface resistance of sample A, the resulting conductivity is relatively flat below 80 K and only starts increasing with decreasing temperature below 70 K. This suggests that the subtraction of a temperature independent residual loss may not be an appropriate way to deal with the residual loss in these crystals, a possibility that will be discussed in more detail in the next section.

Regardless of whether or not a constant surface resistance is subtracted, the conductivity below  $T_c$  increases with decreasing  $T$  to a maximum value of about 20 times its normal state value, peaking at about 32 K, and then falls, roughly linearly, to its value at  $T = 1.2$  K. This large peak in  $\sigma_1(T)$  is strikingly different from the conductivity of a conventional BCS superconductor with a temperature-independent scattering time.<sup>41</sup> It is clearly not a coherence peak, which is not surprising since coherence effects are also not apparent in the temperature dependence of the NMR and NQR spin-lattice relaxation rates.<sup>42</sup> Instead, we argue that the strong rise in the conductivity below  $T_c$  must result from a temperature dependent scattering rate, which drops precipitously below  $T_c$ , much more rapidly than the decrease in the normal fluid density. At the relatively low frequency of the measurements presented here ( $\omega\tau \ll 1$ ),  $\sigma_1(T)$  is roughly proportional to the product  $x_n(T)\tau(T)$  and competition between these two sources of temperature dependence can lead to a peak in the temperature dependence of  $\sigma_1$  and, consequently, in  $R_s$ . Measurements by Nuss *et al.* have revealed a similar peak in  $\sigma_1(T)$  at terahertz frequencies that was also explained in terms of a rapidly falling scattering rate below  $T_c$ .<sup>10</sup> The general trend is for the peak to become smaller and move to higher temperature as the frequency is increased. In addition to the large peak in  $\sigma_1(T)$  the relatively weak (linear) temperature dependence below 30 K is also quite different from the rapid exponential decrease that results from the energy gap in an  $s$ -wave BCS superconductor.

In the next section we elaborate on the “two-fluid”

model which allows us to extract the temperature dependence of  $\tau$  from the temperature dependence of  $\sigma_1$  and  $\lambda$ , and we discuss the connection between this model and BCS theory.

#### IV. EXTRACTING $\tau$ FROM $\lambda$ AND $\sigma_1$

##### A. A generalized two-fluid model

The model which we consider is a generalized two-fluid model for the microwave conductivity of superconductors. The model makes no assumption about the temperature dependence of the superfluid fraction  $x_s(T)$ . In particular it does *not* make the arbitrary assumption of the Gorter-Casimir model that  $x_s \propto 1 - (T/T_c)^4$ . Instead, the temperature dependence is inferred from the penetration depth via Eq. (13).

It is useful to consider the dimensionless function

$$\tilde{\sigma}(\omega) = \tilde{\sigma}_1(\omega) + i\tilde{\sigma}_2(\omega) \equiv \frac{4\pi\omega\sigma(\omega)}{\omega_p^2}, \quad (20)$$

where  $\sigma(\omega)$  is the complex conductivity and  $\omega_p = (4\pi n_0 e^2/m^*)^{1/2}$  is the plasma frequency corresponding to the density,  $n_0$ , of conduction electrons with effective mass  $m^*$ . For a simple Drude metal above  $T_c$  the density of charge carriers is independent of temperature and

$$\tilde{\sigma}(\omega) = \frac{\omega\tau}{1 - i\omega\tau}, \quad (21)$$

where  $\tau$  is the scattering time, is strictly a function of the product  $\omega\tau$ .

We first consider the low frequency behavior of the complex conductivity of BCS superconductors. In a BCS superconductor below  $T_c$ , the function  $\tilde{\sigma}$  will depend not only on  $\tau$  but also on the energy gap  $\Delta$  and on the temperature,  $T$ . The detailed frequency, temperature, and  $\tau$  dependence of the conductivity of weak-coupling superconductors has been derived by Lee and Rainer,<sup>43</sup> using the quasiclassical formalism of energy-integrated Green's functions. The resulting expressions, together with a convenient computer program for evaluating them, are given in a paper by Zimmerman *et al.*<sup>44</sup> Here we consider the limiting case of these expressions (or rather, the corresponding expressions for the functions  $\tilde{\sigma}_1$  and  $\tilde{\sigma}_2$ ), for the “clean” limit,  $\tau\Delta \gg 1$  ( $l \gg \xi_0$ ).

Because of their very short coherence lengths, and the results of far-infrared measurements<sup>4</sup> the high- $T_c$  superconductors are generally thought to be in the clean limit. In the clean limit, and at low frequencies ( $\omega\tau \ll 1$ ), the function  $\tilde{\sigma}_2(\omega, T)$  reflects the temperature dependence of the London penetration depth:

$$\tilde{\sigma}_2(\omega, T) \rightarrow \lambda^2(0)/\lambda^2(T) \quad \text{as } \omega \rightarrow 0. \quad (22)$$

We find that the real part,  $\tilde{\sigma}_1(\omega)$ , has the approximate form

$$\tilde{\sigma}_1(\omega, T, 1/\tau) = x_n(T)f_{\text{BCS}}(\omega\tau, T). \quad (23)$$

The normal fluid fraction,  $x_n(T)$ , can be determined from the superfluid fraction

$$x_s(T) = \frac{\lambda^2(0)}{\lambda^2(T)} = \bar{\sigma}_2(0, T), \quad (24)$$

and the relation  $x_n(T) = 1 - x_s(T)$ .

For a Drude metal above  $T_c$ ,  $x_n(T) = 1$  and

$$\bar{\sigma}_1(\omega, T, 1/\tau) = f_{\text{Drude}}(\omega\tau) \equiv \frac{\omega\tau}{1 + (\omega\tau)^2}. \quad (25)$$

Note that in the Drude case  $f(\omega\tau)$  is only a function of  $\omega\tau$  and temperature dependence can only come into play via a temperature dependent scattering time,  $\tau(T)$ .  $f_{\text{Drude}}(\omega\tau)$  has the following properties.

1. An initial linear slope,  $f_{\text{Drude}}(\omega\tau) \approx \omega\tau$  for  $\omega\tau \ll 1$ ,
2. a broad peak centered at  $\omega\tau = 1$  with a maximum value of  $1/2$ , and
3. a fall-off that approaches  $f_{\text{Drude}}(\omega\tau) \approx (\omega\tau)^{-1}$  for  $\omega\tau \gg 1$ .

In the case of a BCS superconductor below  $T_c$  the function  $f_{\text{BCS}}(\omega\tau, T)$  has a weak temperature dependence in addition to any temperature dependence that might come from  $\tau$ . In principle Eqs. (23) and (24) and our knowledge of the function  $f_{\text{BCS}}(\omega\tau, T)$  would allow us to extract the temperature dependence of  $1/\tau$  (if there is any) from microwave conductivity measurements of a BCS superconductor. The dependence of the function  $f_{\text{BCS}}(\omega\tau)$  for various temperatures and scattering rates is illustrated in Fig. 8. In particular, the function  $f_{\text{BCS}} \equiv \bar{\sigma}_1/x_n$  has the following properties.

1. An initial linear slope with a logarithmic factor,  $f_{\text{BCS}} \sim -\omega\tau \ln(\omega\tau)$  for  $\omega\tau \ll 1$ ,
2. a broad maximum occurring around  $\omega\tau = 1$ , for  $T \approx T_c$  and moving to lower frequency with de-

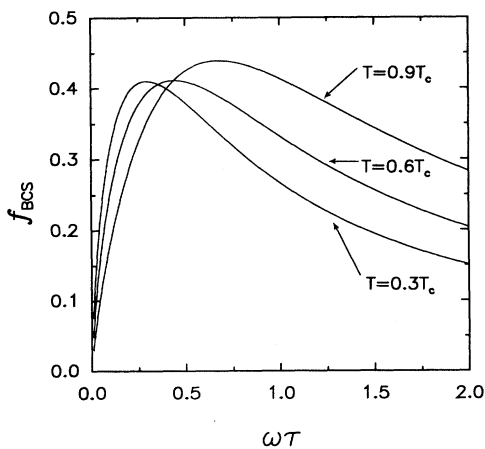


FIG. 8. The function  $f(\omega\tau)$  at various temperatures for a BCS superconductor in the clean limit [ $\hbar/\tau \ll 2\Delta(0)$ ]. The general shape of these curves is only weakly temperature dependent, and the function remains bounded below a value of  $1/2$  at all temperatures.

creasing  $T$ , and

3. a maximum value which is less than or equal to  $1/2$ . The equality holds above  $T_c$  where  $f$  is given by  $f_{\text{Drude}}$  [Eq. (25)].

Despite the fact that the BCS conductivity spectrum, with its logarithmic divergence at low frequency, is different in detail from the Drude spectrum the overall features of  $f_{\text{BCS}}(\omega\tau)$  are similar to the behavior of the Drude form,  $f_{\text{Drude}}(\omega\tau)$ .

We would like to use the generalized two-fluid model to analyze the real and imaginary parts of the conductivity obtained from surface resistance and penetration depth measurements. The temperature dependence of the penetration depth can be used to determine  $x_s$  and consequently  $x_n$ . Then the normalized real part of the conductivity,  $f$ , can be used to estimate the value of  $\tau$  using curves such as those shown in Fig. 8 for  $f_{\text{BCS}}(\omega\tau)$ .

Of course one can imagine numerous pitfalls to such an approach. Leaving aside, for the moment, the question of experimental artifacts, we consider the possibility that the high- $T_c$  superconductor in question may not be an  $s$ -wave BCS superconductor. For example, it could be a  $p$ - or  $d$ -wave superconductor with nodes in the gap, or it could be some other completely different kind of superconductor (anyon, RVB, etc.). In such cases, the analysis described above would yield, at best, an effective scattering time because of the lack of a detailed knowledge of the frequency dependence of the function  $f$ . Given this uncertainty, a plausible approach, which we will adopt, is to interpret the data in terms of

$$\sigma_1(\omega, T) = \frac{c^2}{4\pi\omega\lambda^2(0)} x_n(T) f(\omega\tau), \quad (26)$$

where for simplicity we use the Drude form of  $f(\omega\tau)$  [Eq. (25)] to extract the temperature dependent scattering time. This choice for the form of  $f$  corresponds to diffusive motion of excitations from the condensate and is appropriate for a thermally excited gas of weakly scattered quasiparticles. It completely ignores coherence effects (the log factors) which are characteristic of weak-coupling BCS theory. This approach is justified by the absence of a coherence peak in the NMR spin-lattice relaxation rate<sup>6</sup> data and also by the apparently Drude-like shape of the conductivity found below  $T_c$  in the far-infrared.<sup>11</sup> Ultimately, it will be clear from the analysis in the next section that the temperature dependence of  $1/\tau(T)$  is so dramatic that corrections due to coherence effects or non-Drude forms of  $f(\omega\tau)$  are relatively unimportant.

## B. The temperature dependence of $f(\omega\tau)$ and $1/\tau$

Following the preceding discussion, it is possible to extract the function  $f(\omega\tau)$  from measurements of the temperature dependent surface resistance. One strategy for doing this is as follows.

1. A temperature independent residual loss is subtracted from the measured surface resistance.

2. Assuming local electrodynamics, the real part of the conductivity is extracted from the surface resistance using Eqs. (4)–(9) and the experimentally determined form of  $\lambda(T)$  [Eq. (17)]. A value of 1450 Å has been used for  $\lambda(0)$  and  $T_c$  is fixed at 92.7 K. However the results of the analysis are not very sensitive to these precise values.

3. Using the experimental observations that the normal fluid fraction  $x_n(t)$  varies with temperature as  $t^2$  and that  $\text{YBa}_2\text{Cu}_3\text{O}_{7-\delta}$  is in the clean limit, Eqs. (20) and (23) are used to extract  $f(\omega\tau)$  from the real part of the conductivity.

Figure 9(a) displays the results of this analysis for the two crystals, both of which exhibit a striking increase in  $f(\omega\tau)$  with decreasing temperature. At the low frequency of measurement used here ( $\omega\tau \leq 1$ ) the large increase in  $f(\omega\tau)$  indicates a rapid increase in the quasiparticle scattering time  $\tau(T)$  with decreasing temperature. There are two problematic features in Fig. 9(a) that result from the subtraction of residual loss from the surface resistance. First, the two samples give rather different results in the range  $T \approx 70$  K, the vicinity of the minimum in the surface resistance. As mentioned above, the comparatively weak temperature dependence in this range for sample A results from the larger residual loss subtracted from this sample. Second, at low temperatures  $f(\omega\tau)$  diverges with decreasing temperature, exceeding the upper bound of 0.5 that this function has in the BCS and Drude models. This divergence is easily discerned by noting that the temperature dependence of the conductivity is quite linear below 30 K [Fig. 7(a)]; so, if  $x_n(t)$  varies as  $t^2$ , then  $f(\omega\tau)$  varies as  $t^{-1}$ . The situation is even worse if one does not subtract residual loss from the surface resistance. Then the conductivity linearly approaches a constant at low temperature [Fig. 7(b)] and  $f(\omega\tau)$  diverges as  $t^{-2}$ .

An alternative way of handling the residual loss in the surface resistance measurements is to attribute it to a residual normal fluid fraction that varies from sample to sample. One way to model this is to replace the expression for the normal fluid fraction,  $x_n(t) = t^2$ , used in the foregoing analysis, with

$$x_n(t) = t^2[1 - x_n(0)] + x_n(0), \quad (27)$$

where  $x_n(0)$  is a sample dependent residual normal fluid. The two methods of handling the residual loss are physically distinct. Simply subtracting a constant from the surface resistance implies that the loss is due to something outside of the superconductor, such as a spot of flux or a lossy, insulating dielectric layer on the surface, and that this loss is temperature independent. Using a residual normal fluid density implies that the source of the residual loss is in the bulk of the sample, although it is probably not intrinsic. A source of residual normal fluid density in  $\text{YBa}_2\text{Cu}_3\text{O}_{7-\delta}$  might be twin boundaries, a possibility that is suggested by the observation that the sample with the lowest residual loss that we have yet measured (sample B) was almost twin-free. One further assumption built into the use of Eq. (27) is that the residual normal fluid has the same scattering time as the intrinsic normal fluid.

Figure 9(b) displays the temperature dependence of  $f(\omega\tau)$  that results from employing Eq. (27) as a model for the normal fluid density. The values used for  $x_n(0)$  were 0.015 and 0.005 for samples A and B, respectively. These values of residual normal fluid density keep  $f(\omega\tau)$  bounded below a value of 0.5 and reflect the factor of 3 difference in the residual loss observed in the two crystals. Besides keeping  $f(\omega\tau)$  from diverging, this treatment of the residual loss brings the temperature dependence of  $f(\omega\tau)$  for the two crystals into very good agreement over

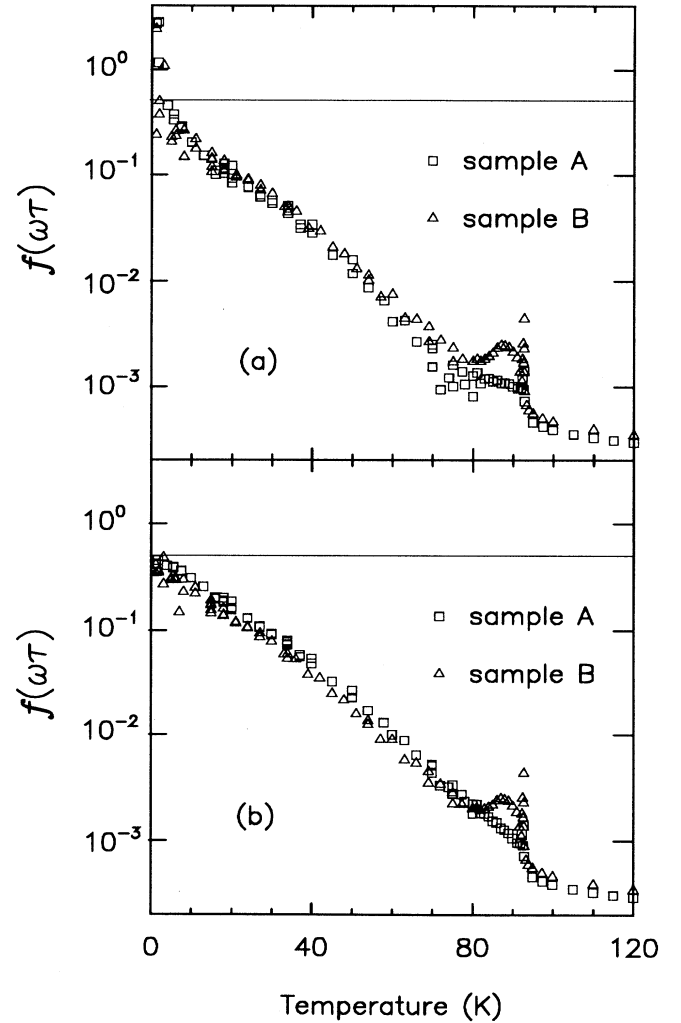


FIG. 9. The function  $f(\omega\tau)$  extracted from the temperature dependent conductivities shown in Fig. 7(a). The rapid increase with decreasing temperature indicates a rapid increase in the lifetime of charge-carrying quasiparticles below  $T_c$ ; (a) is the result of simply subtracting the residual loss from the surface resistance measurements; (b) results from an analysis that assumes that the residual loss comes from a remnant normal fluid density,  $x_n(0)$ , at low temperature.  $x_n(0)$  is chosen to have the minimum value such that  $f(\omega\tau)$  stays below 1/2,  $x_n(0) = 0.005$  and  $0.0015$  for samples A and B, respectively.

the entire temperature range below 84 K. Although these values of  $x_n(0)$  are the minimum ones required to keep  $f(\omega\tau) \leq 1/2$  they generate  $f$ 's that approach  $T = 0$  with nonzero slope, suggesting that somewhat larger values of  $x_n(0)$  might be needed. A plausible maximum value of  $x_n(0)$  is the one that causes  $f(\omega\tau)$  to approach its low temperature value with zero slope. Larger values give rise to a low temperature peak in  $f(\omega\tau)$  that would imply a Kondo-like peak in the scattering rate, a possibility that we will not consider here. By assuming this maximum value of  $x_n(0)$  (0.040 and 0.013 for samples A and B, respectively) the temperature dependence of  $f(\omega\tau)$  is similar for both samples and approaches a low temperature limit of 0.15. The meaning of this is clear if one uses the Drude form for  $f(\omega\tau)$ , Eq. (25), to extract the temperature dependence of  $1/\tau$  from the values of  $f$ . As shown in Fig. 10, the scattering rate below  $T_c$  falls rapidly and then approaches a low temperature limit. The value of  $1/\tau$  above  $T_c$  is  $2.8 \times 10^{13} \text{ s}^{-1}$ , which is in reasonable agreement with the value inferred from far-infrared measurements of thin films,<sup>4</sup> and the low temperature limit is about  $7 \times 10^{10} \text{ s}^{-1}$ , a drop by a factor of 400. So it appears that the strong inelastic scattering responsible for the large dc resistivity of  $\text{YBa}_2\text{Cu}_3\text{O}_{7-\delta}$  is rapidly suppressed below  $T_c$  until  $1/\tau$  reaches a limiting value that is perhaps determined by impurity scattering.

Such a large increase of the scattering time at first seems problematic. For example, if the mean-free path at  $T_c$  is  $l(T_c) \approx 40 \text{ \AA}$ , then the increase in  $\tau$  which we have inferred from our data implies  $l(0) \approx 1.6 \text{ \mu m}$  which is about ten times the assumed value of  $\lambda(0)$ . In an isotropic metal, this would correspond to the anomalous skin effect regime in which carriers can move freely into and out of the region where the field penetrates without scattering from anything but the surface. In such a sit-

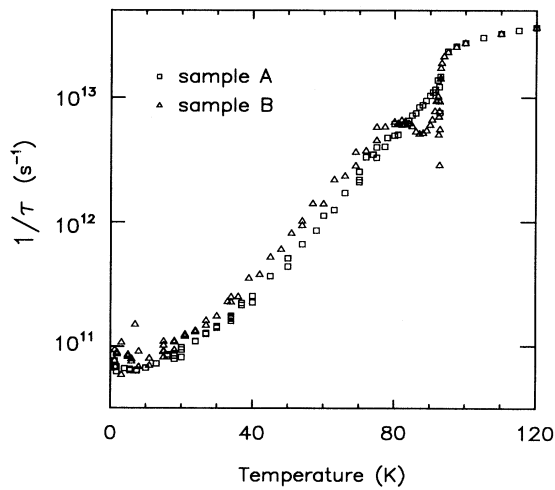


FIG. 10. The temperature dependence of the quasiparticle scattering rate extracted by assuming that the spectral shape of the normal fluid conductivity is Drude-like. The scattering rate falls by a factor of 400 before reaching a limiting value of  $7 \times 10^{10} \text{ s}^{-1}$ , perhaps due to impurity scattering.

uation the response of the charge carriers to an ac field is nonlocal and Eq. (4) no longer applies. However, we should emphasize that the large mean-free path that we find is for motion in the  $ab$  planes. We do not expect large mean-free paths in the  $c$ -axis direction. In fact, on the basis of recent results of Timusk and co-workers on the  $c$ -axis infrared conductivity,<sup>45</sup> we expect the opposite, namely, very short mean-free paths along  $c$ . In this nearly 2D situation local electrodynamics are preserved, even for long mean-free paths in the  $ab$  plane, and Eq. (4) applies even when  $\tau$  is quite large.

We also note that the large increase in  $\tau$  at low temperatures is not sensitive to either the assumed value of  $\lambda(0)$  or to the normalization of  $R_s(T)$ . As noted above,  $\sigma_1(T)$  can be derived quite accurately from Eq. (11) for temperatures more than a few tenths of a Kelvin below  $T_c$ . This means that the temperature dependence of  $\tau$  below 92 K depends only on the measured temperature dependence of  $R_s(T)$  and on the assumed temperature dependence of  $x_n(T)$ :

$$\frac{\tau(T_1)}{\tau(T_2)} = \frac{x_n(T_2)}{x_n(T_1)} \left( \frac{1 - x_n(T_1)}{1 - x_n(T_2)} \right)^{\frac{3}{2}} \frac{R_s(T_1)}{R_s(T_2)}. \quad (28)$$

Thus the two principle sources of uncertainty in this part of the analysis are the assumed temperature dependence of  $x_n(T)$ , particularly at low  $T$ , and the relative temperature dependence of  $R_s(T)$ . With regard to  $R_s(T)$ , a central assumption of this paper is that the temperature dependence of  $R_s(T)$  is, to a good approximation, intrinsic between 20 and 84 K. Below 20 K, there is a residual, sample-dependent loss which we model either as a residual loss or as a residual fraction of normal electrons. Above 84 K, a small peak appears in  $\sigma_1$  and  $\tau$  for sample B which we attribute to some kind of extrinsic broadening of the transition. (On the other hand, the sharp transition observed in sample A may be close to intrinsic behavior.) If the temperature dependent loss which we observe between 20 and 84 K (e.g., the data of Fig. 3) is, in fact, intrinsic, then the rapid drop in  $1/\tau(T)$  which we infer follows directly.

Uncertainty about the detailed temperature dependence of  $x_n(T)$  is rather less of a problem. We find, quite generally that assuming a BCS temperature dependence for  $x_n(T)$  gives unphysical results at low  $T$  because the activated temperature dependence, for any meaningful value of the gap, is too strong. The relatively weak temperature dependence of the observed conductivity can only be reconciled with the strong temperature dependence of the BCS  $x_n(T)$  by using an  $f(\omega\tau)$  with a strong temperature dependence that nearly cancels the BCS contribution. But, there is a limit to this because  $f(\omega\tau)$  is bounded below a value of 1/2, so that a large value of the residual normal fluid density is also needed to suppress the strong BCS form for  $x_n(T)$ . This amounts to including a residual normal fluid density that obscures the activated behavior of the BCS  $x_n(T)$ , which is a rather contrived way of interpreting the experimental conductivity in terms of  $s$ -wave BCS theory. As discussed in detail in Sec. III B a wide variety of measurements that have been analyzed by us and by others<sup>12,32</sup> give

a weaker quadratic temperature dependence of  $x_n(T)$ . Such a power-law dependence for  $x_n(T)$  with small values of  $x_n(0)$  provides a more reasonable way to interpret the weak temperature dependence of  $\sigma_1$  at low temperatures.

In summary we find that

1. The linear temperature dependence of the surface resistance and conductivity below 30 K cannot easily be reconciled with the exponential temperature dependence expected for an *s*-wave BCS energy gap.

2. The nonmonotonic temperature dependence of the surface resistance, which we take to be intrinsic, results from two competing sources of temperature dependence: the normal fluid fraction decreases, but the scattering time of that normal fluid increases with decreasing temperature.

3.  $1/\tau(T)$  is found to fall by roughly a factor of 400 between  $T_c$  and 15 K.

## V. DISCUSSION AND CONCLUSIONS

In this paper we have presented microwave surface resistance measurements on two very high quality  $\text{YBa}_2\text{Cu}_3\text{O}_{6.95}$  crystals which are representative of four that we have studied. These crystals exhibit very sharp drops of about 4 orders of magnitude in surface resistance below  $T_c$  and temperature dependent low temperature loss that peaks around 38 K and then falls off gradually to low residual losses at  $T = 1.2$  K of 2 to 6  $\mu\Omega/\square$ . We have argued that at least most of this temperature dependent surface resistance is an intrinsic loss associated with thermal excitations from the superconducting condensate.

We assume that the surface resistance is related to the complex conductivity by Eqs. (4)–(8). Using Eq. (9) the imaginary part of the conductivity can be determined by the London penetration depth which we have obtained from a careful analysis of recent microwave and  $\mu\text{sr}$  measurements. These measurements show that there is still substantial temperature dependence left in  $\lambda(T)$  even below  $T_c/3$ . This temperature dependence is, to a good approximation, quadratic. The microwave data of Anlage and Langley and of Pond *et al.* is well fit by the relation  $\lambda^2(0)/\lambda^2(T) = 1 - (T/T_c)^2$  for  $7 \text{ K} < T < T_c$ . The temperature dependence of  $\lambda(T)$  found in the  $\mu\text{sr}$  measurements described in Sec. III B are also consistent with this quadratic temperature dependence.

With the imaginary part of the conductivity determined by  $\lambda(T)$ , the real part can be extracted directly from the surface resistance measurements. This analysis shows that the behavior of  $R_s(T)$  is due to a conductivity with a large peak at 32 K and a weak (roughly linear) temperature dependence below the peak. This weak temperature dependence of  $\sigma_1(T)$  below  $T_c/3$  and the power-law temperature dependence of  $\lambda^{-2}(T)$  in the same temperature range provide strong evidence for the existence of low-lying states in the superconducting phase below  $T_c$ . These two quantities provide complementary information.  $\sigma_1(T)$  depends on the temperature dependence of the normal fluid density and  $\lambda(T)$  depends on

the superfluid density. The energy gap of an *s*-wave BCS superconductor leads to a rapid, exponential decrease in normal fluid density below  $T_c/3$  and a superfluid density that quickly reaches its low temperature value and becomes rather temperature independent below  $T_c/3$ . In  $\text{YBa}_2\text{Cu}_3\text{O}_{6.95}$  the relatively slow decrease in  $\sigma_1(T)$  below 30 K and the fact that  $\lambda(T)$  has substantial temperature dependence in this low temperature range both indicate that the normal fluid density does not have the exponential, activated behavior expected for an *s*-wave BCS superconductor. Instead, these measurements both suggest a density of states that extends down to zero energy. Either the spectrum of excitations from the superconducting condensate is gapless or it has a gap structure with nodes. As the present measurements have been performed on twinned crystals, it cannot yet be determined to what extent this behavior is influenced by the anisotropy in the *ab* plane associated with the presence of CuO chains.

Equation (26) provides the basis for deriving the temperature dependence of the scattering rate,  $1/\tau(T)$ , from the real part of  $\sigma$  in terms of the normal fluid density  $x_n(T)$  and the function  $f(\omega\tau)$  for which we assume a simple Drude form, Eq. (25). Below  $T_c$ , the temperature dependent scattering rate derived from our data decreases by nearly 3 orders of magnitude before reaching a low temperature limit of roughly  $7 \times 10^{10} \text{ s}^{-1}$ . The temperature dependent part of the scattering rate can be examined by subtracting the low temperature limiting value from the measured scattering rate before plotting it on a semi-log graph. As shown in Fig. 11, this procedure uncovers an overall exponential behavior for

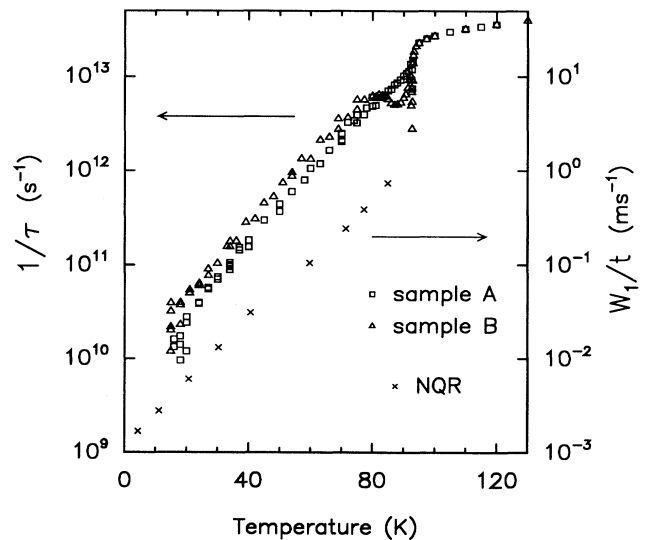


FIG. 11. The temperature dependent part of the quasi-particle scattering rate obtained by subtracting the low temperature limiting value,  $7 \times 10^{10} \text{ s}^{-1}$ , from the curves shown in Fig. 10. The nearly straight line on a semi-log scale indicates a scattering rate that varies as  $\exp(T/T_0)$ , a temperature dependence that is also seen in NMR and NQR measurements (Ref. 6).

the temperature dependent part of the scattering rate;  $1/\tau(T) \propto e^{T/T_0}$ . The value of  $T_0$  depends somewhat on the choices made for the parameter  $x_n(0)$  and ranges between 12 and 14 K. This unusual exponential behavior is not the activated temperature dependence,  $e^{-T_0/T}$ , that one might obtain for a spectrum of scatterers with a gap. A comparison of this to NMR and NQR relaxation rates reveals a striking similarity. Barrett *et al.* noted that all measurements of the relaxation rate, denoted  $W_{1\alpha}$  ( $\alpha = a, b, c$  for magnetic fields applied along the three principle axes of the crystal), follow the same exponential behavior,  $W_{1\alpha}/T \propto e^{T/T_0}$ , with similar values of  $T_0$ .<sup>6</sup> NQR measurements compare most simply to the microwave measurements because they are performed in zero magnetic field. The NQR measurements of Barrett *et al.* are included in Fig. 11 where it is clear that  $1/\tau(T)$  follows an exponential behavior that is similar to  $W_{1c}/T$ .

Since the unusual exponential behavior of  $1/\tau(T)$  is not the activated behavior expected for a spectrum of scatterers with a gap, it must result from inelastic scattering by excitations whose spectrum extends down to rather low energies. So, we find that both the current-carrying excitations from the superconducting condensate and the excitations that scatter this normal fluid have spectra with states extending down to low energies. We would emphasize, however, that the scatterers which damp the current-carrying excitations are almost certainly not just those excitations themselves. This is clear from Eq. (26) which says that  $\sigma_1(T)$  depends on the product of  $x_n(T)$  and  $\tau(T)$ . If the scattering is due to charged excitations whose density is  $x_n(T)$ , then this temperature dependence should cancel out in the product  $x_n(T)\tau(T)$  and the resulting conductivity would be only weakly temperature dependent. Experimentally we

find that  $\sigma_1(T)$  increases rapidly below  $T_c$ , reaching a peak around 32 K which is 20 times its value at  $T_c$ . Thus it would appear that some other kind of excitation is responsible for damping the current and that these other excitations freeze out below  $T_c$  more quickly than the normal "electrons." A good candidate for these other excitations would be antiferromagnetic spin fluctuations which are also responsible for nuclear spin relaxation. This may also account for the identical temperature dependence of the two rates.

We should also note that preliminary measurements in our lab of the surface resistance of similar high quality crystals at 35 GHz are completely consistent with the lower frequency results described above. In addition, we have measured the high field vortex viscosity,  $\eta(T)$ , of superconducting Bi 2:2:1:2 crystals. We find a temperature dependence for  $\eta(T)$  similar to that found above for  $\tau(T)$ , as one would expect from Bardeen-Stephen theory.<sup>46</sup> Both the 35 GHz and vortex viscosity measurements will be published elsewhere.

#### ACKNOWLEDGMENTS

We have benefited from many helpful discussions with T. Timusk, D.B. Tanner, G. Grüner, and P.C.E Stamp. We would also like to acknowledge useful conversations and communications with B. Statt, P.W. Anderson, S. Anlage, J.A. Annett, N. Goldenfeld, R.B. Laughlin, and M.J. Rice. We thank S.M. Anlage and B.W. Langley for sending us their phase velocity data, along with good advice about how to interpret it, and S. Martindale for permission to reproduce the NQR data. This work was supported by grants from the Natural Sciences and Engineering Research Council of Canada and by the Canadian Institute for Advanced Research.

<sup>1</sup>J.G. Bednorz and K.A. Müller, *Z. Phys. B* **64**, 189 (1986).

<sup>2</sup>P.W. Anderson, *Phys. Rev. Lett.* **60**, 132 (1988).

<sup>3</sup>T. Timusk and D.B. Tanner, in *Physical Properties of High Temperature Superconductors I*, edited by D.M. Ginsberg (World Scientific, Singapore, 1989), p. 339.

<sup>4</sup>K. Kamarás, S.L. Herr, C.D. Porter, N. Tache, D.B. Tanner, S. Etemad, T. Venkatesan, E. Chase, A. Inam, X.D. Wu, M.S. Hegde, and B. Dutta, *Phys. Rev. Lett.* **64**, 84 (1990).

<sup>5</sup>H. Monien, P. Monthoux, and D. Pines, *Phys. Rev. B* **43**, 275 (1991).

<sup>6</sup>S.E. Barrett, J.A. Martindale, D.J. Durand, C.H. Pennington, C.P. Slichter, T.A. Friedmann, J.P. Rice, and D.M. Ginsberg, *Phys. Rev. Lett.* **66**, 108 (1991), and references cited therein.

<sup>7</sup>A.J. Millis, M. Monien, and D. Pines, *Phys. Rev. B* **42**, 176 (1990).

<sup>8</sup>S.-W. Cheong, G. Aeppli, T.E. Mason, H. Mook, S.M. Hayden, P.C. Canfield, Z. Fisk, K.N. Clausen, and J.L. Martinez, *Phys. Rev. Lett.* **67**, 1791 (1991), and references cited therein.

<sup>9</sup>M.J. Rice and Y.R. Wang, *Bull. Amer. Phys. Soc.* **34**, 517 (1989); and (unpublished).

<sup>10</sup>Martin C. Nuss, P.M. Mankiewich, M.L. O'Malley, E.H. Westerwick, and Peter B. Littlewood, *Phys. Rev. Lett.* **66**, 3305 (1991).

<sup>11</sup>D.B. Romero, C.D. Porter, D.B. Tanner, L. Forro, D. Mandrus, L. Mihaly, G.L. Carr, and G.P. Williams, *Phys. Rev. Lett.* **68**, 1590 (1992).

<sup>12</sup>J.M. Pond, K.R. Carroll, J.S. Horowitz, D.B. Chrisey, M.S. Osofsky, and V.C. Cestone, *Appl. Phys. Lett.* **59**, 3033 (1991).

<sup>13</sup>Ruixing Liang, P. Dosanjh, D.A. Bonn, D.J. Baar, J.F. Carolan, and W.N. Hardy, *Physica C* **195**, 51 (1992).

<sup>14</sup>P. Schleger, W.N. Hardy, and B.X. Yang, *Physica C* **176**, 261 (1991).

<sup>15</sup>D.A. Bonn, D.C. Morgan, and W.N. Hardy, *Rev. Sci. Instrum.* **62**, 1819 (1991).

<sup>16</sup>T.A. Friedman, J.P. Rice, John Giapintzakis, and D.M. Ginsberg, *Phys. Rev. B* **39**, 4258 (1991).

<sup>17</sup>D. Baar, Ruixing Liang, and W.N. Hardy (unpublished).

<sup>18</sup>L.G. Aslamazov and A.I. Larkin, *Fiz. Tverd. Tela (Leningrad)* **10**, 1104 (1968) [*Sov. Phys. Solid State*, **10**, 875 (1968)].

<sup>19</sup>D.A. Bonn, P. Dosanjh, R. Liang, and W.N. Hardy, *Phys.*

- Rev. Lett. **68**, 2390 (1992).
- <sup>20</sup>Dong-Ho Wu, W.L. Kennedy, C. Zahopoulos, and S. Sridhar, Appl. Phys. Lett. **55**, 696 (1989).
- <sup>21</sup>D.L. Rubin, K. Green, J. Gruschus, J. Kirchgessner, D. Moffat, H. Padamsee, J. Sears, Q.S. Shu, L.F. Schneemeyer, and J.V. Waszczak, Phys. Rev. Lett. **38**, 6538 (1988).
- <sup>22</sup>J. Halbritter, Z. Phys. **266**, 209 (1974).
- <sup>23</sup>C. Kittel, *Quantum Theory of Solids* (Wiley, New York, 1963); J.R. Waldram, Adv. Phys. **13**, 1 (1964).
- <sup>24</sup>M. Tinkham, in *Far Infrared Properties of Solids*, edited by S.S. Mitra and S. Nudelman (Plenum, New York, 1974), p. 223.
- <sup>25</sup>B.W. Langley, S.M. Anlage, R.F.W. Pease, and M.R. Beasley, Rev. Sci. Instrum. **62**, 1801 (1991).
- <sup>26</sup>S.M. Anlage, B.W. Langley, G. Deutcher, J. Halbritter, and M.R. Beasley, Phys. Rev. B **44**, 9764 (1991).
- <sup>27</sup>L. Kruisin-Elbaum, R.L. Greene, F. Holtzberg, A.P. Malozemoff, and Y. Yeshurun, Phys. Rev. Lett. **62**, 217 (1989).
- <sup>28</sup>A.T. Fiory, A.F. Hebard, P.M. Mankiewich, and R.E. Howard, Phys. Rev. Lett. **61**, 1419 (1988).
- <sup>29</sup>D.R. Harshman, L.F. Schneemeyer, J.V. Waszczak, G. Aeppli, R.J. Cava, B. Batlogg, L.W. Rupp, E.J. Ansaldo, and D.Ll. Williams, Phys. Rev. B **39**, 851 (1989).
- <sup>30</sup>B. Pümpin, H. Keller, W. Kündig, W. Odermatt, I.M. Šavić, J.W. Schneider, H. Simmler, P. Zimmermann, J.G. Bednorz, Y. Maeno, K.A. Müller, C. Rossel, E. Kaldis, S. Rusiecki, W. Assmus, and J. Kowalewski, Physica C **151-152**, 151 (1989).
- <sup>31</sup>F. Gross, B.S. Chandrasekhar, D. Einzel, K. Andres, P.J. Hirschfeld, H.R. Ott, J. Beuers, Z. Fisk, and J.L. Smith, Z. Phys. B **64**, 175 (1986).
- <sup>32</sup>J.A. Annett, N. Goldenfeld, and S.R. Renn, Phys. Rev. B **39**, 2778 (1991).
- <sup>33</sup>S.M. Anlage and D.-H. Wu, J. Supercond. **5**, 395 (1992).
- <sup>34</sup>S.S. Laderman, R.C. Taber, R.D. Jacowitz, J.L. Moll, C.B. Eom, T.L. Hylton, A.F. Marshall, T.H. Geballe, and M.R. Beasley, Phys. Rev. B **43**, 2922 (1991); D. Miller *et al.*, Appl. Phys. Lett. **59** 2326 (1991); J. Halbritter, J. Appl. Phys. **71**, 1 (1992).
- <sup>35</sup>E.H. Brandt, J. Low Temp. Phys. **73**, 355 (1988).
- <sup>36</sup>A.D. Siderenko, V.P. Smilga, and V.I. Fesenko, Hyperfine Int. **63**, 49 (1990).
- <sup>37</sup>P.H. Kobrin, J.T. Cheung, W.W. Ho, N. Glass, J. Lopez, I.S. Gergis, R.E. DeWames, and W.F. Hall, Physica **C176**, 121 (1991).
- <sup>38</sup>O. Klein, K. Holczer, and G. Grüner, Phys. Rev. Lett. **68**, 2407 (1992).
- <sup>39</sup>K. Holczer, L. Forro, L. Mihály, and G. Grüner, Phys. Rev. Lett. **67**, 152 (1991).
- <sup>40</sup>N.E. Glass and W.F. Hall, Phys. Rev. B **44**, 4495 (1991).
- <sup>41</sup>F. Marsiglio, Phys. Rev. B **44**, 5373 (1991).
- <sup>42</sup>P.C. Hammel, M. Takigawa, R. H. Heffner, Z. Fisk, and K.C. Ott, Phys. Rev. Lett. **63**, 1992 (1989).
- <sup>43</sup>W. Lee and D. Rainer, Physica C **159**, 535 (1989).
- <sup>44</sup>W. Zimmerman, E.H. Brandt, M. Bauer, E. Seider, and L. Genzel, Physica **C183**, 99 (1991).
- <sup>45</sup>C.C. Homes, N. Cao, T. Timusk, Ruixing Liang, and W.N. Hardy (unpublished).
- <sup>46</sup>J. Bardeen and M.J. Stephen, Phys. Rev. **140**, A1197 (1963).